AIAA JOURNAL
Vol. 47, No. 1, January 2009

Nonlinear Constitutive Relations of Cellular Materials

Lin-Hua Lan* and Ming-Hui Fu†
Sun Yat-Sen University, 510275 Guangzhou, Guangdong Province, People's Republic of China

DOI: 10.2514/1.39531

The nonlinear constitutive relations of the cellular materials are presented in this paper based on the large deformation analysis of elastic beams in plane. The relations reflect the dependences of equivalent stress, equivalent Young's modulus, equivalent Poisson's ratio, and equivalent shear modulus on the deformation. It is found that the modified factors of the linear constitutive relations are associated with the shape and deformation of a considered cellular material and independent of the ratio of the face thickness t to length l (t/l) of the material. So the constitutive relations can describe the mechanical properties of the cellular materials with the same shape.

Nomenclature

As	=	area of the cross section
b	=	face breadth of honeycomb
E	=	equivalent Young's modulus of honeycomb
E_{HC}	=	initial equivalent Young's modulus of honeycomb
E_s	=	Young's modulus of the honeycomb material
e	=	Almansi strain
G_{xy}	=	equivalent shear modulus of honeycomb
h	=	vertical face length of honeycomb
$\bar{h}$	=	projected length of vertical face along y direction
I	=	second moment of the cross section
k_1, k_2, m_1, m_2, α	=	modified factors of the linear constitutive relations of honeycomb
l	=	slanting face length of honeycomb
M	=	bending moment
P	=	force
P_{cr}	=	critical force
R	=	relative density of honeycomb
S	=	nondimensional curvilinear coordinate
s	=	curvilinear coordinate
t	=	face thickness of honeycomb
U_{sub}	=	projected length of the face sub along x direction
V_{sub}	=	projected length of the face sub along y direction
$\bar{X}$	=	nondimensional projected length of slanting face along x direction
$\bar{Y}$	=	nondimensional projected length of slanting face along y direction
β	=	rotation angle at point C
γ_{xy}	=	shear strain
θ	=	angle between the slanting face and x direction
μ	=	equivalent Poisson's ratio of honeycomb
ξ	=	nondimensional force
σ	=	Euler stress
τ	=	shear stress
Φ	=	angle between the slanting face and y direction

Received 3 July 2008; revision received 15 September 2008; accepted for publication 17 September 2008.

*Ph.D. Student, Department of Applied Mechanics and Engineering; whoswod@163.com.

†Professor, Department of Applied Mechanics and Engineering stsfmh@mail.sysu.edu.cn (Corresponding Author).

I. Introduction

THE cellular materials (Fig. 1), or honeycombs, have been used in a wide range of applications due to their excellent properties, such as a high stiffness-to-weight ratio, high strength-to-weight ratio, low thermal conductivity, and good sound insulating capacity. Many man-made honeycombs are used to make light, stiff structures (such as skis and aircraft panels) or to absorb energy (in packaging). More general three-dimensional cellular materials (foams) are widely used in the applications when strength and low weight are both required. A variety of materials are now available as cellular structures. Aluminium, paper, and "Nomex" honeycombs are made by expanding bonded sheet material [1]. Usually the cellular materials are in separate forms, and so they are regarded as anisotropic materials.

Many researchers have studied the mechanical properties of the honeycombs in the past three decades. The earliest cellular materials equivalent model was given by Abd El-Sayed et al. [2]. They analyzed the in-plane Young's modulus of honeycombs and the collapse stress when plastic hinges form at the ends of faces. They obtained the result that the initial equivalent Young's modulus of a regular honeycomb E_{HC} was isotropic in the plane and was related to the ratio of the face thickness t to length l (t/l) by

$$E_{\mathrm{HC}} = \frac{4}{\sqrt{3}} E_s \left(\frac{t}{l}\right)^3 \tag{1}$$

For low-density regular honeycombs of uniform face thickness, the relative density R is given by

$$R = \frac{2}{\sqrt{3}} \left(\frac{t}{l}\right) \tag{2}$$

And so the initial Young's modulus of a regular honeycomb is only related to its relative density by

$$E_{\mathrm{HC}} = 1.5 E_s R^3 \tag{3}$$

Gibson et al. [3] and Gibson and Ashby [4] confirmed Abd El-Sayed et al.'s results, extended their analysis, and established clearly constitutive relations of the honeycombs by

$$\begin{aligned} E_1^* &= E_s \frac{t^3}{l^3} \frac{\cos\theta}{(h/l + \sin\theta)\sin^2\theta} \qquad \nu_1^* = \frac{\cos^2\theta}{(h/l + \sin\theta)\sin\theta} \\ E_2^* &= E_s \frac{t^3}{l^3} \frac{(h/l + \sin\theta)}{\cos^3\theta} \qquad \nu_2^* = \frac{(h/l + \sin\theta)\sin\theta}{\cos^2\theta} \\ G_{xy}^* &= E_s \frac{t^3}{l^3} \frac{(h/l + \sin\theta)}{(h/l)^2(2h/l + 1)\cos\theta} \end{aligned} \tag{4}$$

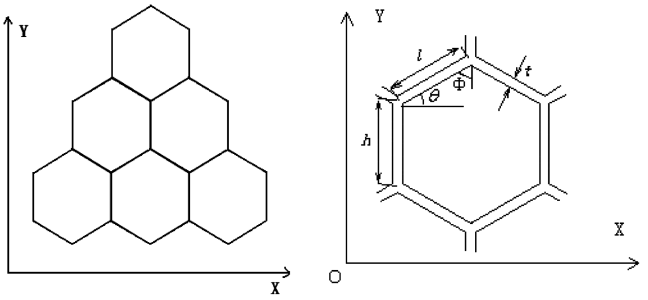

Fig. 1 Hexagonal honeycomb structure (left) and its unit cell (right).

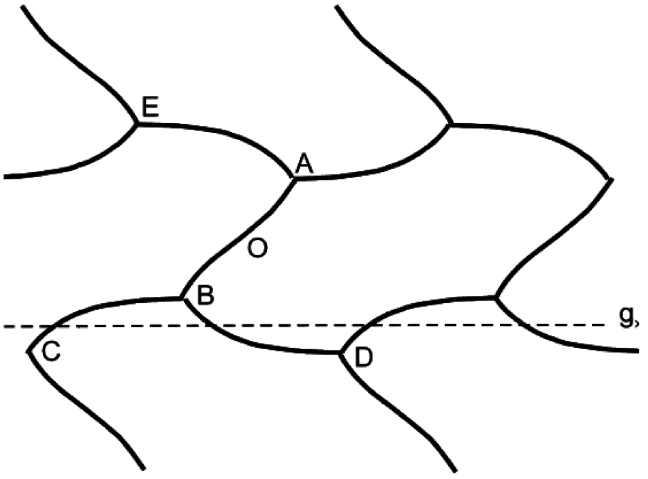

Fig. 2 Compression of a honeycomb in the *y* direction, with neighboring vertices rotating in opposite directions. The glide plane in the *x* direction is shown as a dashed line.

These formulas have a simple form and can be applied expediently. They are related by the reciprocal relation

$$E_1\nu_2 = E_2\nu_1 \tag{5}$$

Warren and Kraynik [5] and Fu and Yin [6] modified Gibson's formula by considering the axial deformation of the slanting faces which increased the precision of the analysis and enlarged its application scope when the honeycomb endures complicated stress. Papka and Kyriakides [7] presented the results of finite element analysis (FEA) for the compression of an aluminum honeycomb with double-thickness vertical faces. Both elastic and elastic–plastic material were considered. In their experiments on aluminum honeycomb, neighboring vertices were observed rotating in opposite directions when high-strain deformation occurred (Fig. 2). They also studied the mechanical response of circular-cell honeycomb under uniaxial loading in one direction [8] and extended their work to investigate the response to biaxial loading [9,10]. Warren et al. [11] investigated the mechanical response of honeycomb by considering the geometrically nonlinear deformation of units which consisted of three honeycomb half-faces joined at 120 deg at a vertex. Mills and Zhu [12] studied the deformation mechanisms for the high-strain compression polystyrene foams and found these foams significantly different from those in an aluminum honeycomb. Hutzler and Weaire [13] analyzed the biaxial in-plane compression of honeycombs by using an energy approach and presented an elastic buckling pattern which was similar to that in Fig. 2.

Chung and Waas [14–16] did extensive research work to investigate the mechanical properties of circular cell and elliptical cell honeycombs. They studied the crushing response of a polycarbonate circular cell honeycomb to in-plane biaxial loading, and both static and dynamic experiments' results were presented. The results were then simulated through numerical analysis using the finite element method. Through several comparisons between the experimental and numerical results, the biaxial in-plane crushing mechanisms of circular cell honeycombs were presented.

Zhu and Mills [17] analyzed the in-plane uniaxial compression of regular honeycomb from a range of materials, considering both material and geometric nonlinearity. They compared the effects of varying material parameters on the elastic and plastic collapse of honeycombs with different densities and found that their effects of each on the shape of the stress-strain curve can be separated. Their method and the method in the current investigation are essentially the same, but they did not analyze the in-plane expansion or shear behavior of the honeycomb. The goals of this paper are to find the nonlinear constitutive relations of the cell materials with the same shape by analyzing the in-plane deformation of the honeycombs.

II. Analysis of In-Plane Deformation

A. Analysis of In-Plane Tension or Compression Deformation

1. Analysis of In-Plane Tension of the Slanting Face in the y Direction

When a honeycomb is uniaxial tensioned in the *y* direction, there is no vertex rotation because of the symmetry of the structure and the loading. So the deformation of the slanting face *AB* is shown in Fig. 3a. The bending moment at midpoint *C* of the slanting face is zero. Thus, analyzing only the shape of the half-face *AC* is enough. The moment distribution in *AC* is the same as if it were a cantilever beam. The free end *C* is loaded by the force *P* acting in the *y* direction, Fig. 3b. The governing differential equation for it is given by

$$E_s I \frac{\mathrm{d}^2\gamma}{\mathrm{d}s^2} = -P\sin(\phi - \gamma) \tag{6}$$

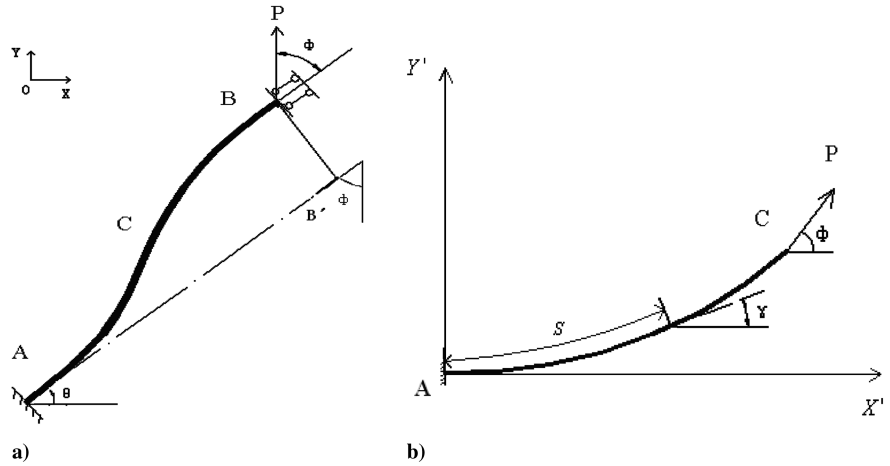

Fig. 3 Uniaxial tension in the *y* direction of the slanting face.

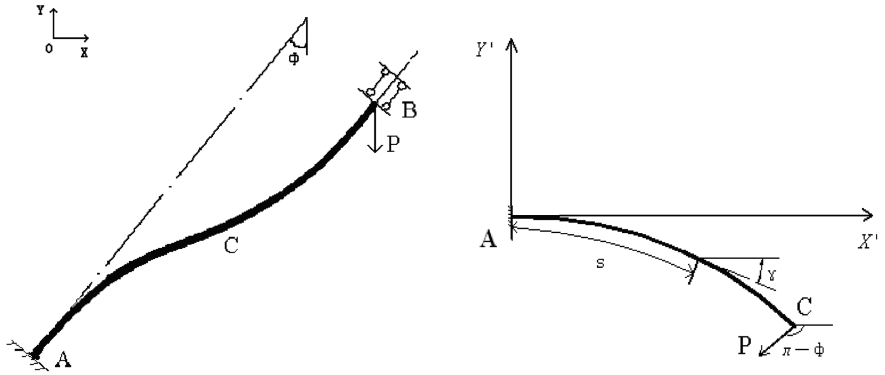

Fig. 4 Uniaxial compressed in the *y* direction of the slanting face.

where E_s is the Young's modulus of the honeycomb material, and I is the second moment of the cross section. s is the curvilinear coordinate with origin at A, the angle of rotation measured counterclockwise at a general point on the face, and Φ is the angle between the vertical face and the slanting face of the honeycomb, a constant for a specific honeycomb. The boundary condition is

$$M(A) = 0 \tag{7}$$

The governing differential equation (6) is turned into a nondimensional equation by

$$\frac{\mathrm{d}^2\gamma}{\mathrm{d}S^2} = -\xi^2\pi^2 \sin(\phi - \gamma) \tag{8}$$

where

$$\xi = \sqrt{\frac{P}{P_{\mathrm{cr}}}}$$

$$P_{\mathrm{cr}} = \frac{\pi^2 E_s I}{l^2}$$

and $S = s/l (0 \le S \le 0.5)$.

For a long, thin strut the deflections due to shear or axial deformation can be neglected compared with those due to bending [18]. The nondimensional force ξ then can be described by an elliptical integral

$$\xi = \frac{2}{\pi}F(\beta) = \frac{2}{\pi}\int_{\eta_0}^{\pi/2} \frac{1}{\sqrt{1 - \cos^2(\phi/2 - \beta/2)\sin^2\eta}}\,\mathrm{d}\eta \tag{9}$$

where β is the value of γ at C, the lower limit of integration is

$$\eta_0 = \sin^{-1}\left[\frac{\cos(\phi/2)}{\cos(\phi/2 - \beta/2)}\right] \tag{10}$$

and η is defined by

$$\sin\eta = \frac{\cos(\phi/2 - \gamma/2)}{\cos(\phi/2 - \beta/2)} \tag{11}$$

The face orientation Φ is 60 deg for regular honeycombs, but the result applies when the hexagon cell angles are not 120 deg.

The nondimensional projected length of the face AB along the x (the direction perpendicular to the force) and y axes (parallel to the force) is given by

$$\bar{X} = \frac{2}{F(\beta)}\cos(\phi/2 - \beta/2)\cos\eta_0 \qquad \bar{Y} = 1 - \frac{2E(\beta)}{F(\beta)} \tag{12}$$

where $E(\beta)$ is also an elliptic integral

$$E(\beta) = \int_{\eta_0}^{\pi/2} \sqrt{1 - \cos^2(\phi/2 - \beta/2)\sin^2\eta}\,\mathrm{d}\eta \tag{13}$$

For a given initial β, increased by small steps, the nondimensional force ξ, and projected lengths $\bar{X}$ and $\bar{Y}$ can be calculated from Eqs. (9) and (12).

The moment at A can also be determined from Eqs. (7) and (8) by

$$M(A) = E_s I \left.\frac{\mathrm{d}\gamma}{\mathrm{d}S}\right|_{\gamma=0} = 2\sqrt{2}EsIF(\beta)\sqrt{\cos(\phi - \beta) - \cos\phi} \tag{14}$$

2. Analysis of In-Plane Deformation of the Slanting Face in Other Directions

Zhu and Mills [17] analyzed the honeycomb uniaxial compressed in the y direction (Fig. 4) with and without vertex rotation. Here, it is assumed there is no vertex rotation due to the symmetry of the structure and the loading. The replacement of ϕ with $(\pi + \Phi)$ in Eq. (6) will produce the results which will be used in the analysis of the in-plane shear model.

When honeycomb is uniaxial tensioned or compressed in the x direction, the analysis is similar to that for the in-plane deformation in the y direction, but the initial orientation of face AC relative to the force P is $(\pi/2 - \Phi)$ for uniaxial tension and $(3\pi/2 - \Phi)$ for uniaxial compression. So replacing ϕ with them in Eq. (6) can get the results expediently. It is noticeable that the nondimensional projected lengths $\bar{X}$ and $\bar{Y}$ should be switched in the end.

3. Nonlinear Constitutive Relations of the Honeycomb

Here the superscripts $'$ and $''$ are used to represent the force applied along the x and y axes on the honeycomb, with both tension and compression included.

Thus the Euler stresses are given by

$$\sigma_x' = \frac{P}{b(l\bar{Y}' + h)} = \frac{\pi^2\xi^2 E_s t^3}{12(\bar{Y}' + h/l)l^3}, \qquad \sigma_y' = 0$$
$$\sigma_x'' = 0, \qquad \sigma_y'' = \frac{P}{bl\bar{X}''} = \frac{\pi^2\xi^2 E_s t^3}{12\bar{X}''l^3} \tag{15}$$

where b is the face breadth of the honeycomb.

The Almansi strains which depend on the projected length are given by

$$e_x' = \frac{\bar{X}' - \sin\phi}{\bar{X}'} - \frac{1}{2}\left(\frac{\bar{X}' - \sin\phi}{\bar{X}'}\right)^2$$
$$e_y' = \frac{\bar{Y}' - \cos\phi}{\bar{Y}' + h/l} - \frac{1}{2}\left(\frac{\bar{Y}' - \cos\phi}{\bar{Y}' + h/l}\right)^2$$
$$e_x'' = \frac{\bar{X}'' - \sin\phi}{\bar{X}''} - \frac{1}{2}\left(\frac{\bar{X}'' - \sin\phi}{\bar{X}''}\right)^2 \tag{16}$$
$$e_y'' = \frac{\bar{Y}'' - \cos\phi}{\bar{Y}'' + \bar{h}/l} - \frac{1}{2}\left(\frac{\bar{Y}'' - \cos\phi}{\bar{Y}'' + \bar{h}/l}\right)^2$$

where $\bar{h}$ is the projected length of vertical face along the y axis given by

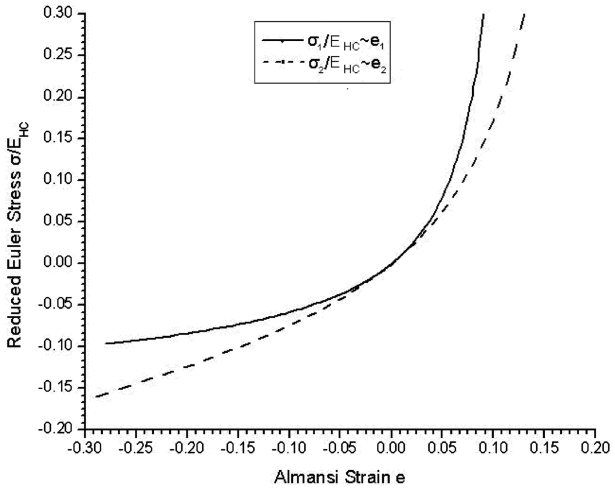

Fig. 5 The reduced Euler stress vs the Almansi strain relationship for the regular honeycomb, loaded in the *x* direction (solid line) and the *y* direction (dashed line). Both tension and compression are considered.

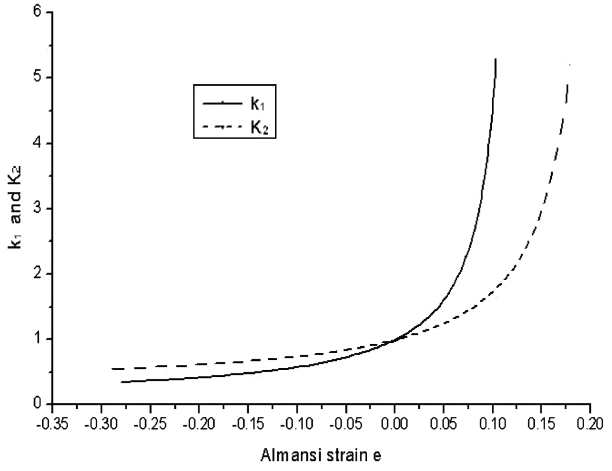

Fig. 6 The modified factors of the equivalent Young's modulus (k_1 and k_2) vs the Almansi strain relationship for the regular honeycomb, loaded in the *x* and *y* directions. Both tension and compression are considered.

$$\bar{h} = h \pm 2Ph/E_s A_s = h\left(1 \pm \frac{\pi^2 \xi^2 t^2}{6l^2}\right) \tag{17}$$

where $A_s = bt$ is the area of the cross section of the face.

The equivalent Young's modulus and equivalent Poisson's ratio are given by

$$\begin{aligned} E_1 &= \sigma_x'/e_x' = k_1 E_1^* \qquad \nu_1 = -e_y'/e_x' = m_1 \nu_1^* \\ E_2 &= \sigma_y''/e_y'' = k_2 E_2^* \qquad \nu_2 = -e_x''/e_y'' = m_2 \nu_2^* \end{aligned} \tag{18}$$

where E_1^*, ν_1^*, E_2^*, and ν_2^* are given by Eq. (4), and k_1, m_1, k_2, and m_2 are the modified factors of the linear constitutive relations given by

$$k_1 = \frac{\pi^2 \xi^2 \bar{X}'^2 \sin^2\theta (h/l + \sin\theta)}{6(\bar{Y}' + h/l)(\bar{X}'^2 - \sin^2\phi)\cos\theta}$$

$$m_1 = -\frac{\bar{X}'^2(\bar{Y}'^2 + 2\bar{Y}'h/l - 2\cos\phi h/l - \cos^2\phi)(h/l + \sin\theta)\sin\theta}{(\bar{Y}' + h/l)^2(\bar{X}'^2 - \sin^2\phi)\cos^2\theta}$$

$$k_2 = \frac{\pi^2 \xi^2 \cos^3\theta (\bar{Y}'' + \bar{h}/l)^2}{6\bar{X}''(h/l + \sin\theta)(\bar{Y}''^2 + 2\bar{Y}''\bar{h}/l - 2\cos\phi\bar{h}/l - \cos^2\phi)}$$

$$m_2 = -\frac{(\bar{Y}'' + \bar{h}/l)^2(\bar{X}''^2 - \sin^2\phi)\cos^2\theta}{\bar{X}''^2(\bar{Y}''^2 + 2\bar{Y}''\bar{h}/l - 2\cos\phi\bar{h}/l - \cos^2\phi)(h/l + \sin\theta)\sin\theta} \tag{19}$$

These four factors are dependent on the shape and deformation of the honeycomb, but are not related to the relative density R.

The response of a typical steel regular honeycomb was simulated. To make the results applicable for any relative density R of honeycomb, the reduced Euler stress is defined as the honeycomb stress divided by the honeycomb Young's modulus E_{HC}. Figure 5 shows that the relationship between the reduced Euler stress and the Almansi strain is nonlinear when the strains exceed 4% of tension and 4.5% of compression. The initial slopes of the graphs are 1.0, as required. Here, both tension and compression are included.

Figure 6 shows the variation of the modified factors (k_1 and k_2) with the Almansi strain, where both tension and compression are considered. k_1 is the modified factor of Young's modulus loaded in the *x* direction with k_2 loaded in the *y* direction. Both k_1 and k_2 have a value of 1.0 for small strains, increase monotonically with the honeycomb tension strain, and decrease with the compression strain, which means the capability of the honeycomb to resist tension is getting better, while the capability to resist compression is getting worse, which is an important property of the honeycombs. Also, Fig. 6 shows that k_1 is larger than k_2 for the tension situation and smaller than k_2 for compression, which means the capability of resist tension in the *x* direction is better than that in the *y* direction, while the *y* direction is better than the *x* direction for compression.

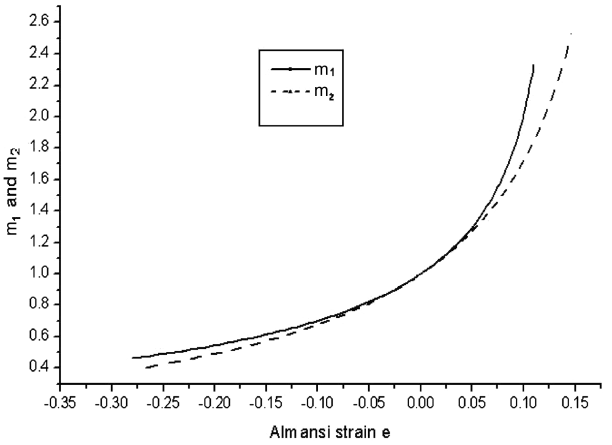

Fig. 7 The modified factors of the equivalent Poisson's ratio (m_1 and m_2) vs the Almansi strain relationship for the honeycomb. The solid line means loaded in the *x* direction and the dashed line in the *y* direction. Both tension and compression are considered.

Figure 7 shows the modified factors (m_1 and m_2) vs the Almansi strain curve for the honeycombs, where four cases of loading are considered. All of them have a value of 1 for small strains, which means the equivalent Poisson's ratio is equal to Gibson's result for small strains. Both m_1 and m_2 increase monotonically with the tension strain and decrease with compression strain. m_1 is slightly larger than m_2 at the same strain indicating the strain along the *y* axis is relatively high.

B. Analysis of In-Plane Shear Deformation

The analysis of in-plane shear deformation is shown in Fig. 8. The faces *AB* and *BC* will become *S* shaped of different size when the force *F* is applied at point *D* and the length between their midpoint ($\overline{A'C'}$) is a constant, which is $\overline{AC}/2$. The moment at A' and C' is zero due to the antisymmetry of the structure and the loading. Thus only the shapes of three half-faces will be analyzed (Fig. 8b). They can be regarded as three cantilever half-faces bending under the forces F, F_1, and F_2. Hence the previously results still apply here.

In Fig. 8b, β, β_1, β_2, and β_3 are rotation angles at points B, A', C', and D. ϕ_1 is the angle between F_1 and the original orientation of face BA', and ϕ_2 is the angle between F_2 and BC'. M_1, M_2, and M_3 are the moments of faces $A'B$, $C'B$, and DB at point B; the arrows show the

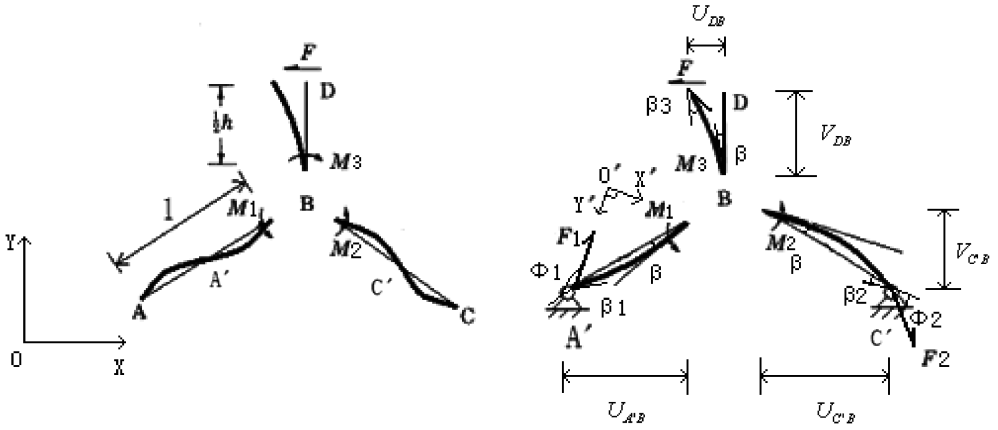

a) b)

Fig. 8 Cell deformation under shear stress.

directions of positive moments on the faces. $U_{A'B}$, $V_{A'B}$, $U_{C'B}$, $V_{C'B}$, U_{DB}, and V_{DB} are the projected lengths along the x and y directions of faces $A'B$, $C'B$, and DB. ξ_1, ξ_2, and ξ_3 are the nondimensional forces of F_1, F_2, and F by

$$\xi_i = \sqrt{\frac{F_i}{P_{\text{cr}i}}} \tag{20}$$

where

$$F_3 = F, \qquad P_{\text{cr1}} = P_{\text{cr2}} = \frac{\pi^2 E_s I}{l^2}$$

$$P_{\text{cr3}} = \frac{\pi^2 E_s I}{h^2}$$

In the next analysis, β, β_1, β_2, β_3, ϕ_1, and ϕ_2 are basic variables, and all of the other variables can be expressed using them. The question is how to construct equations from the equilibrium and harmonious conditions.

1. Analysis of Three Half-Faces

For face $A'B$, the results can be gained from Sec. II.A.1 as follows:
The nondimensional force is given by

$$\xi_1 = \frac{2}{\pi} F_1(\beta_1, \phi_1, \beta) = \frac{2}{\pi}\int_{\eta_1}^{\pi/2} \frac{1}{\sqrt{1-\cos^2(\phi_1/2+\beta/2-\beta_1/2)\sin^2\eta}}\,\mathrm{d}\eta \tag{21}$$

where the lower limit of integration is

$$\eta_1 = \sin^{-1}\left[\frac{\cos(\phi_1/2+\beta/2)}{\cos(\phi_1/2+\beta/2-\beta_1/2)}\right] \tag{22}$$

The moment at B is given by

$$M_1 = EsI\left.\frac{\mathrm{d}\gamma}{\mathrm{d}S}\right|_{\gamma=0} = 2\sqrt{2}EsIF_1(\beta_1,\phi_1,\beta)\sqrt{\cos(\phi_1+\beta-\beta_1)-\cos(\phi_1+\beta)} \tag{23}$$

The projected length of face $A'B$ along the x and y axes is given by

$$\begin{aligned} U_{A'B} &= lX_{A'B}\sin(\theta+\phi_1) + lY_{A'B}\cos(\theta+\phi_1) \\ V_{A'B} &= lX_{A'B}\cos(\theta+\phi_1) + lY_{A'B}\sin(\theta+\phi_1) \end{aligned} \tag{24}$$

where θ is the angle between the original orientation of face $A'B$ and the x axis, and $X_{A'B}$ and $Y_{A'B}$ are nondimensional projected lengths of face $A'B$ along the x' (the direction perpendicular to F_1) and the y' axes (parallel to F_1). They can be determined from Eq. (12) by

$$\begin{aligned} X_{A'B} &= \frac{1}{F_1(\beta_1,\phi_1,\beta)}\cos(\phi_1/2+\beta/2-\beta_1/2)\cos\eta_1 \\ Y_{A'B} &= 0.5 - \frac{E_1(\beta_1,\phi_1,\beta)}{F_1(\beta_1,\phi_1,\beta)} \\ &= 0.5 - \frac{\int_{\eta_1}^{\pi/2}\sqrt{1-\cos^2(\phi_1/2+\beta/2-\beta_1/2)\sin^2\eta}\,\mathrm{d}\eta}{F_1(\beta_1,\phi_1,\beta)} \end{aligned} \tag{25}$$

Similarly, for face $C'B$, replacing the subscript can produce the following results:
The nondimensional force is given by

$$\xi_2 = \frac{2}{\pi}F_2(\beta_2,\phi_2,\beta) = \frac{2}{\pi}\int_{\eta_2}^{\pi/2}\frac{1}{\sqrt{1-\cos^2(\phi_2/2+\beta/2-\beta_2/2)\sin^2\eta}}\,\mathrm{d}\eta \tag{26}$$

where the lower limit of integration is

$$\eta_2 = \sin^{-1}\left[\frac{\cos(\phi_2/2+\beta/2)}{\cos(\phi_2/2+\beta/2-\beta_2/2)}\right] \tag{27}$$

The moment at B is given by

$$M_2 = 2\sqrt{2}EsIF_2(\beta_2,\phi_2,\beta)\sqrt{\cos(\phi_2+\beta-\beta_2)-\cos(\phi_2+\beta)} \tag{28}$$

The projected length of face $C'B$ along the x and y axes is given by

$$\begin{aligned} U_{C'B} &= lX_{C'B}\sin(\theta+\phi_2) + lY_{C'B}\cos(\theta+\phi_2) \\ V_{C'B} &= lX_{C'B}\sin(\theta+\phi_2) + lY_{A'B}\cos(\theta+\phi_2) \end{aligned} \tag{29}$$

where $X_{A'B}$ and $Y_{A'B}$ are nondimensional projected lengths of face $C'B$ along the direction perpendicular to F_2 and the direction parallel to F_2. They are given by

$$\begin{aligned} X_{C'B} &= \frac{1}{F_2(\beta_2,\phi_2,\beta)}\cos(\phi_2/2+\beta/2-\beta_2/2)\cos\eta_2 \\ Y_{C'B} &= 0.5 - \frac{E_2(\beta_2,\phi_2,\beta)}{F_2(\beta_2,\phi_2,\beta)} \\ &= 0.5 - \frac{\int_{\eta_2}^{\pi/2}\sqrt{1-\cos^2(\phi_2/2+\beta/2-\beta_2/2)\sin^2\eta}\,\mathrm{d}\eta}{F_2(\beta_2,\phi_2,\beta)} \end{aligned} \tag{30}$$

The results for face DB are as follows:
The nondimensional force is given by

$$\xi_3 = \frac{2l}{\pi h} F_3(\beta_3, \beta) = \frac{2l}{\pi h} \int_{\eta_3}^{\pi/2} \frac{1}{\sqrt{1 - \cos^2(\pi/4 - \beta/2 - \beta_3/2)\sin^2\eta}} \, d\eta \quad (31)$$

where the lower limit of integration is

$$\eta_3 = \sin^{-1}\left[\frac{\cos(\pi/4 - \beta/2)}{\cos(\pi/4 - \beta/2 - \beta_3/2)}\right] \quad (32)$$

The moment at B is

$$M_3 = 2\sqrt{2} EsIF_3(\beta_3, \beta)\sqrt{\sin(\beta + \beta_3) - \sin\beta} \quad (33)$$

The projected length of DB along the x and y axes is given by

$$U_{DB} = \frac{h}{F_3(\beta_3, \beta)} \cos(\pi/4 - \beta/2 - \beta_3/2)\cos\eta_3$$
$$V_{DB} = \frac{h}{2} - \frac{E_3(\beta_3, \beta)}{F_3(\beta_3, \beta)} \cdot h = \frac{h}{2} - \frac{\int_{\eta_3}^{\pi/2} \sqrt{1 - \cos^2(\pi/4 - \beta/2 - \beta_3/2)\sin^2\eta}\, d\eta}{F_3(\beta_3, \beta)} \cdot h \quad (34)$$

2. Equilibrium and Harmonious Conditions

Notice $U_{A'B} + U_{C'B} = \overline{A'C'} = l * \cos\theta$ and $V_{A'B} = V_{C'B}$, which can determine two equations from Eqs. (24) and (29)

$$X_{A'B}\sin(\theta + \phi_1) + Y_{A'B}\cos(\theta + \phi_1) + X_{C'B}\sin(\theta + \phi_2) + Y_{C'B}\cos(\theta + \phi_2) - \cos\theta = 0 \quad (35)$$

$$X_{A'B}\cos(\theta + \phi_1) + Y_{A'B}\sin(\theta + \phi_1) - X_{C'B}\sin(\theta + \phi_2) - Y_{A'B}\cos(\theta + \phi_2) = 0 \quad (36)$$

By $M_1 + M_2 = M_3$, Eq. (37) can be given from Eqs. (23), (28), and (33) by

$$\xi_1\sqrt{\cos(\phi_1 - \beta) - \cos(\phi_1 - \beta + \beta_1)} + \xi_2\sqrt{\cos(\phi_2 + \beta - \beta_2) - \cos(\phi_2 + \beta)} - \xi_3\sqrt{\sin(\beta + \beta_3) - \sin\beta} = 0 \quad (37)$$

Otherwise, from the equilibrium of the cell unit (Fig. 8b) along the x and y axes, Eqs. (38) and (39) are determined by

$$\xi_1\cos(\phi_1 + \theta) + \xi_2\cos(\phi_2 + \theta) - \xi_3 = 0 \quad (38)$$

$$\xi_1\sin(\phi_1 + \theta) - \xi_2\sin(\phi_2 + \theta) = 0 \quad (39)$$

For the given nondimensional force ξ_3 that increased in small steps, the basic variables β, β_1, β_2, β_3, ϕ_1, and ϕ_2 can be calculated from Eqs. (31) and (35–39), which construct a closed solution system using the Newton–Raphson numeric algorithm. In the calculation, the initial values of basic variables for the first force step are given by the linear solution, and the solutions of basic variables are used for the initial values of basic variables of the second force step. The process is then repeated, and finally the solutions of basic variables for every force step can be determined by the Newton–Raphson iterative method. Thus the other variables can also be determined.

3. Nonlinear Constitutive Relation of the Honeycomb

The equivalent shear stress is given by

$$\tau = F/2lb\cos\theta = \frac{\xi_3^2\pi^2 E_s}{24\cos\theta}\left(\frac{t}{l}\right)^3 \quad (40)$$

where b is the breadth of the face.

The equivalent shear strain is given by

$$\gamma_{xy} = \frac{\partial u}{\partial y} = \frac{U_D}{(V_{DB} + V_{A'B})} \quad (41)$$

where U_D is the placement of point D along the x axis.

Then, the shear modular determined from $G_{xy} = \tau/\gamma_{xy}$ is given by

$$G_{xy} = \frac{\xi_3^2\pi^2 E_s(V_{DB} + V_{A'B})}{24\cos\theta U_D}\left(\frac{t}{l}\right)^3 \quad (42)$$

which can be written in an alternative form by

$$G_{xy} = \alpha G_{xy}^* \quad (43)$$

where G_{xy}^* is given by Eq. (4), and α is the modified factor given by

$$\alpha = \frac{\xi_3^2\pi^2(V_{DB} + V_{A'B})(h/l)^2(2h/l + 1)}{24U_D(h/l + \sin\theta)} \quad (44)$$

It also depends on the shape and deformation of the honeycomb but is not related to the relative density R determined by Eq. (2).

Figure 9 shows the variation of the reduced shear stress with the shear strain for the regular honeycomb. To make the results applicable for any relative density R of a honeycomb, the reduced shear stress is also defined as the honeycomb shear stress divided by the honeycomb Young's modulus E_{HC}. The solid line is this paper's result, and the dashed line is Gibson et al.'s linear result [3]. The current results coincide with Gibson's results for small strain, and the solid line is larger than the dashed line for high strain, which means the honeycombs' shear property is getting better compared with the initial linear honeycomb.

Figure 10 shows the modified factor of the shear modulus α vs the shear strain γ_{xy} curve for different kinds of honeycombs ($\Phi = 30, 45, 60$, and 75 deg). For all four honeycombs, the modified factors α increase monotonically with the honeycomb strains and have values of 1 for small strains. Also, for a certain strain, the modified factor α with larger Φ is smaller than that with smaller Φ. The modified factor α also depends on the shape and deformation of the honeycomb and is not related to the ratio of the face thickness t and length l, which is similar to the properties of the modified factors k_1, m_1, k_2, and m_2.

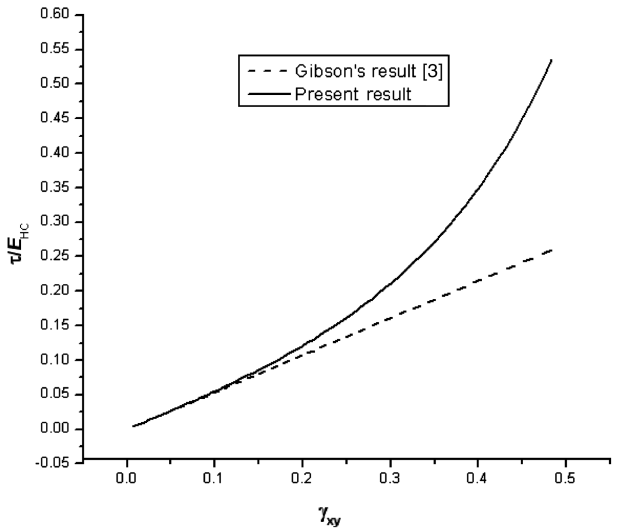

Fig. 9 The relation between the reduced shear stress and the shear strain γ_{xy} for regular honeycombs.

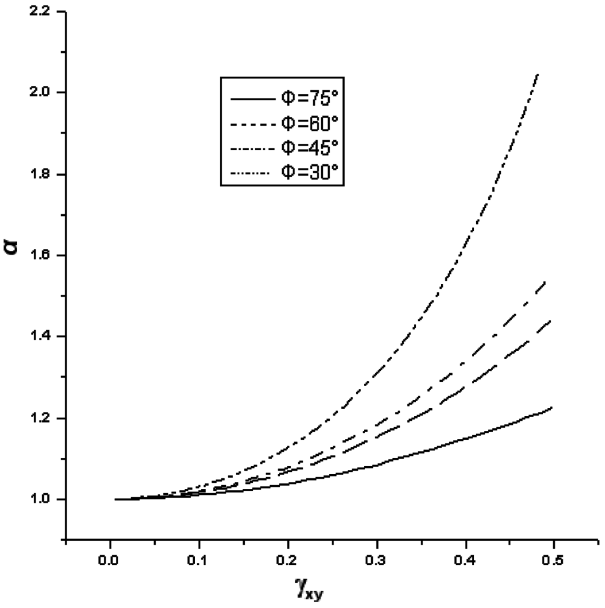

Fig. 10 The modified factor of the shear modulus and the shear strain γ_{xy} relationship for different kinds of honeycombs.

III. Conclusions

First, based on the elastic bending theory of beams in large deflection, a theoretical analysis method about the nonlinear constitutive relations is performed. This method is based on solving a series of determined equations, and so it has better precision than a separated method such as FEA.

Second, the modified factors of the linear constitutive relations are produced. All of them are dependent on the shape and deformation of the cellular materials and not related to the ratio of the face thickness t and length l (t/l). So they can reflect mechanical properties of a kind of honeycombs (with the same shape but different value of t/l).

Acknowledgments

This work was supported by the National Natural Science Foundation of China (Grant No. 10672194) and by the Guang Dong Province Natural Science Foundation of China (Grant No. 031552).

References

[1] Bitzer, T., *Honeycomb Technology*, Chapman and Hall, London, 1997.

[2] Abd El-Sayed, F. K., Jones, R., and Burgess, I. W., "A Theoretical Approach to the Deformation of Honeycomb Based Composite Materials," *Composites*, Vol. 10, No. 4, 1979, pp. 209–214. doi:10.1016/0010-4361(79)90021-1

[3] Gibson, L. J., Ashby, M. F., Schiajer, G. S., and Robertson, C. I., "The Mechanics of Two-Dimension Cellular Materials," *Proceedings of the Royal Society of London A*, Vol. A382, No. 1782, 1982, pp. 25–42. doi:10.1098/rspa.1982.0087

[4] Gibson, L. J., and Ashby, M. F., *Cellular Solids, Structure and Properties*, Pergamon, Oxford, England, U.K., 1988.

[5] Warren, W. E., and Kraynik, A. M., "Foam Mechanics: The Linear Elastic Response of Two-Dimensional Spatially Periodic Cellular Materials," *Mechanics of Materials*, Vol. 6, No. 1, 1987, pp. 27–37. doi:10.1016/0167-6636(87)90020-2

[6] Fu, M.-H., and Yin, J.-R., "Equivalent Elastic Parameters of the Honeycomb Core," *Acta Mechanica Sinica*, Vol. 31, No. 1, 1999, pp. 113–118 (in Chinese).

[7] Papka, S. D., and Kyriakides, S., "In-Plane Compressive Response and Crushing of Honeycomb," *Journal of the Mechanics and Physics of Solids*, Vol. 42, No. 10, 1994, pp. 1499–1532. doi:10.1016/0022-5096(94)90085-X

[8] Papka, S. D., and Kyriakides, S., "In-Plane Crushing of a Polycarbonate Honeycomb," *International Journal of Solids and Structures*, Vol. 35, Nos. 3–4, 1998, pp. 239–267. doi:10.1016/S0020-7683(97)00062-0

[9] Papka, S. D., and Kyriakides, S., "Biaxial Crushing of Honeycombs—Part 1: Experiments," *International Journal of Solids and Structures*, Vol. 36, No. 29, 1999, pp. 4367–4396. doi:10.1016/S0020-7683(98)00224-8

[10] Papka, S. D., and Kyriakides, S., "In-Plane Biaxial Crushing of Honeycombs—Part 2: Analysis," *International Journal of Solids and Structures*, Vol. 36, No. 29, 1999, pp. 4397–4423. doi:10.1016/S0020-7683(98)00225-X

[11] Warren, W. E., Kraynik, A. M., and Stone, C. M., "A Constitutive Model for Two-Dimensional Non-Linear Elastic Foams," *Journal of the Mechanics and Physics of Solids*, Vol. 37, No. 6, 1989, pp. 717–733. doi:10.1016/0022-5096(89)90015-X

[12] Mills, N. J., and Zhu, H. X., "The High Strain Compression of Closed-Cell Polymer Foams," *Journal of the Mechanics and Physics of Solids*, Vol. 47, No. 3, 1999, pp. 669–695. doi:10.1016/S0022-5096(98)00007-6

[13] Hutzler, S., and Weaire, D., "Buckling Properties of 2D Regular Elastic Honeycombs," *Journal of Physics: Condensed Matter*, Vol. 9, No. 22, 1997, pp. L323–L329. doi:10.1088/0953-8984/9/22/002

[14] Chung, J., and Waas, A. M., "The Inplane Elastic Properties of Circular Cell and Elliptical Cell Honeycombs," *Acta Mechanica*, Vol. 144, Nos. 1–2, 2000, pp. 29–42. doi:10.1007/BF01181826

[15] Chung, J., and Waas, A. M., "Compressive Response of Circular Cell Polycarbonate Honeycombs Under Inplane Biaxial Static and Dynamic Loading—Part 1: Experiments," *International Journal of Impact Engineering*, Vol. 27, No. 7, 2002, pp. 729–754. doi:10.1016/S0734-743X(02)00011-8

[16] Chung, J., and Waas, A. M., "Compressive Response of Circular Cell Polycarbonate Honeycombs Under Inplane Biaxial Static and Dynamic Loading—Part 2: Simulations," *International Journal of Impact Engineering*, Vol. 27, No. 10, 2002, pp. 1015–1047. doi:10.1016/S0734-743X(02)00012-X

[17] Zhu, H. X., and Mills, N. J., "The In-Plane Non-Linear Compression of Regular Honeycombs," *International Journal of Solids and Structures*, Vol. 37, No. 13, 2000, pp. 1931–1949.

[18] Timoshenko, S., and Gere, J., *Theory of Elastic Stability*, McGraw–Hill, New York, 1961.

A. Palazotto
Associate Editor